JOURNAL OF VIROLOGY, June 1997, p. 4736–4743 Vol. 71, No. 6
0022-538X/97/$04.00+0

Coxsackievirus A21 Binds to Decay-Accelerating Factor but Requires Intercellular Adhesion Molecule 1 for Cell Entry

DARREN R. SHAFREN,[1]* DOUGLAS J. DORAHY,[2] REBECCA A. INGHAM,[1] GORDON F. BURNS,[2] AND RICHARD D. BARRY[1]

Department of Microbiology[1] and Cancer Research Unit,[2] Faculty of Medicine, The University of Newcastle, Newcastle, New South Wales 2300, Australia

Received 11 December 1996/Accepted 3 March 1997

It is becoming increasingly apparent that many viruses employ multiple receptor molecules in their cell entry mechanisms. The human enterovirus coxsackievirus A21 (CAV21) has been reported to bind to the N-terminal domain of intercellular adhesion molecule 1 (ICAM-1) and undergo limited replication in ICAM-1-expressing murine L cells. In this study, we show that in addition to binding to ICAM-1, CAV21 binds to the first short consensus repeat (SCR) of decay-accelerating factor (DAF). Dual antibody blockade using both anti-ICAM-1 (domain 1) and anti-DAF (SCR1) monoclonal antibodies (MAbs) is required to completely abolish binding and replication of high-titered CAV21. However, the binding of CAV21 to DAF, unlike that to ICAM-1, does not initiate a productive cell infection. The capacity of an anti-DAF (SCR3) MAb to block CAV21 infection but not binding, coupled with immunoprecipitation data from chemical cross-linking studies, indicates that DAF and ICAM-1 are closely associated on the cell surface. It is therefore suggested that DAF may function as a low-affinity attachment receptor either enhancing viral presentation or providing a viral sequestration site for subsequent high-affinity binding to ICAM-1.

Virus-cell receptor interactions are a major determinant of viral host range specificity, and the identification of specific viral receptors has greatly increased our understanding of viral pathogenesis. However, in recent years it has become appreciated that viral cell attachment and subsequent transfer of viral genomes across the cell membrane are frequently more complex events than previously thought. Several viruses have now been shown to enter cells via receptor complexes rather than by individual cell surface molecules. Virus-receptor complexes are postulated to consist of distinct virus attachment and virus internalization components; e.g., human immunodeficiency virus can bind to human CD4 (27) or galactosyl ceramide (3) but requires the coexpression of the chemokine receptor fusin (15, 24) or CC-CKR-5 (13, 14) for cell entry, and adenovirus type 2 attaches to cells via an unknown primary receptor but requires the presence of integrin αvβ3/β5 for cell entry (41). Measles viruses can bind either to membrane cofactor protein CD46 or to the membrane-organizing external spike protein moesin; coexpression of both molecules results in a more productive infection (37). The cell attachment and internalization of the human enterovirus coxsackievirus B3 (CVB3) is thought to employ a receptor complex consisting of decay-accelerating factor (DAF; CD55) and an as yet unidentified 49.5-kDa protein (2, 11, 38).

Against this background, we questioned whether coxsackievirus A21 (CAV21) requires multiple receptor molecules to initiate productive cell infection. CAV21, a human picornavirus, is a known causal agent of upper respiratory infections and considered to be a possible recombinant between poliovirus and rhinovirus (21). CAV21 shares a cellular attachment receptor with the major group rhinoviruses: intercellular adhesion molecule 1 (ICAM-1) (7, 26, 39). Recently, we have shown that anti-ICAM-1 domain 1 monoclonal antibodies (MAbs) can block CAV21 replication in HeLa-B cells at a low virus input multiplicity (10^2 50% tissue culture infective doses [$TCID_{50}$]/well) (39). However, the present study was initiated by the finding that anti-ICAM-1 (domain 1) MAbs only partially blocked CAV21 lytic infection at higher CAV21 input multiplicities (10^3 to 10^4 $TCID_{50}$/well), suggesting that additional cellular receptors may be involved in CAV21 cell entry.

Recently, DAF has been identified as a cell attachment receptor for a number of hemagglutinating enteroviruses (1, 2, 6, 22, 38, 40). DAF is a complement regulatory protein ubiquitously expressed on most mammalian cells, including erythrocytes, and consists of four tandem copies of an approximately 60-amino-acid structural motif, containing conserved cysteine, proline, glycine, phenylalanine/tyrosine, and tryptophan residues, termed short consensus repeat (SCR) (33). Following the four SCRs, the molecule possesses a serine/tyrosine-rich region of approximately 70 amino acids, followed by a carboxyl-terminal domain that acts as the signal for the attachment of a glycosylphosphatidylinositol anchor (33). The human enteroviruses echovirus type 7 (E7) and CBV3 bind to a region which is on or near the third SCR of the DAF molecule (1, 2, 6, 38). As CAV21 has been reported to agglutinate erythrocytes (20) and to have its replication blocked by a MAb raised against a HeLa cell surface protein that also blocks the replication of a number of hemagglutinating enteroviruses (11), we investigated whether DAF was involved in CAV21 cell attachment and entry.

Here we show that CAV21 binds to DAF as well as ICAM-1. Complete antibody blockade of virus binding to cells expressing both receptors required the combined use of MAbs to both DAF and ICAM-1. Interestingly, blocking of viral binding with a panel of anti-DAF MAbs showed that, uniquely among DAF-binding enteroviruses described to date, CAV21 binds to SCR1. However, although both DAF and ICAM-1 appear to cooperate in viral binding, our experiments indicate that ICAM-1 expression is required for the completion of a successful CAV21 lytic infection.

* Corresponding author. Mailing address: Discipline of Pathology, Faculty of Medicine, Level 3, David Maddison Clinical Sciences Building, Royal Newcastle Hospital, Newcastle, New South Wales 2300, Australia. Phone: 61 49 23 6158. Fax: 61 49 23 6814. E-mail: dshafren@medicine-dmb.newcastle.ed.au.

MATERIALS AND METHODS

Cells and viruses. E7 (Wallace), poliovirus type 2 (Sabin) (PV2), and CVA21 (KuyKendall) were obtained from Margery Kennett, Enterorespiratory Laboratory, Fairfield Hospital, Melbourne, Victoria, Australia. Human rhinovirus type 14 (HRV14) was obtained from the American Type Culture collection. All viruses were grown in HeLa-B cells. Rhabdomyosarcoma (RD) and HeLa-B cells were obtained from Margery Kennett; HEp2 cells were obtained from the Commonwealth Serum Laboratories, Parkville, Victoria, Australia; and Chinese hamster ovary (CHO) and CHO-DAF cells were obtained from Bruce Loveland, Austin Research Institute, Heidelberg, Victoria, Australia. COS cells were obtained from Andrew Boyd, Walter and Elisa Hall Institute, Melbourne, Victoria, Australia.

Antibodies. The anti-ICAM-1 MAb WEHI (4) was obtained from Andrew Boyd. The anti-DAF MAbs IA10, VIIIA7, and IIH6 (23) were generous gifts from Taroh Kinoshita, Department of Immunoregulation, Osaka University, Osaka, Japan, and MAb IH4 (9) was obtained from Bruce Loveland. The anti-poliovirus receptor (PVR) MAb 280 (30) was supplied by Philip Minor, National Institute of Biological Standards and Control, Potters Bar, United Kingdom. The anti-CD36 MAb VM58 (28) and anti-VLA2 MAb (AK7) were obtained from Michael Berndt, The Baker Institute, Melbourne, Victoria, Australia.

Radiolabeled virus binding assays. Viruses were radiolabeled in Dulbecco's modified essential medium (DMEM) containing [^{35}S]methionine and purified by velocity centrifugation in 5 to 30% sucrose gradients as previously described (38). HEp2, HeLa-B, and RD cell monolayers in 24-well plates were preincubated with MAbs (20 μg), washed, and then incubated with radiolabeled viruses (2×10^4 to 5×10^4 cpm) in serum-free DMEM for 1 h at 37°C. Following three washes, the cell monolayers were dissolved in 200 μl of 0.2 M NaOH–1.0% sodium dodecyl sulfate (SDS), and the amount of labeled virus bound was measured by liquid scintillation counting.

For virus binding assays following phosphatidylinositol-specific phospholipase C (PI-PLC) treatment, cells were removed from monolayers by using an EDTA solution, resuspended in DMEM containing 1.0% bovine serum albumin and 150 μM 2-mercaptoethanol, and divided into two portions, one of which received PI-PLC (1.0 U per 5×10^6 cells) (Sigma Chemicals, Sydney, New South Wales Australia). Both cell suspensions were incubated at 37°C for 1 h and then washed, and 4×10^5-cell aliquots were placed into Eppendorf tubes prior to incubation with radiolabeled virus.

Virus infectivity assay. Cell monolayers in 96-well plates were inoculated with 50 μl of serial dilutions of the viruses for 1 h at 37°C, then 200 μl of DMEM containing 1.0% fetal calf serum (DMEM-FCS) was added to each well, and the plates were incubated at 37°C for 48 h. To quantitate cell survival, monolayers were incubated with a crystal violet-methanol solution and washed with distilled water, and the plates were read on a multiscan enzyme-linked immunosorbent assay plate reader (Flow Laboratories) at a wavelength of 540 nm. Fifty percent endpoint titers were calculated by the method of Reed and Muench (34), where a well was scored as positive if its absorbance was less than the no-virus control minus 3 standard deviations (SD).

For assessing MAb blockade of virus-mediated cell lysis, cell monolayers in 96-well plates were incubated with 50 μl of MAb (20 μg/ml) for 1 h at 37°C prior to the addition of 10^4 $TCID_{50}$ CAV21 and quantitation of cell lysis by the procedure described above.

For cell lysis assays with PI-PLC treatment, monolayers of transfected RD cells in microtiter plates were incubated with either DMEM-FCS [(−) PI-PLC cells] or DMEM-FCS containing PI-PLC at 1.0 U per 5×10^6 cells [(+) PI-PLC cells] for 1 h at 37°C. The cell monolayers were then washed with phosphate-buffered saline (PBS), and 50-μl aliquots of the stock viral dilutions were added to the appropriate wells. Following incubation at 37°C for 1 h, 50 μl of DMEM-FCS was added to each well of the (−) PI-PLC cells, while 50 μl of DMEM containing PI-PLC (1.0 U per 5×10^6 cells) was added to each well of the (+) PI-PLC cells. Microtiter plates were then incubated for 24 h at 37°C, and cell survival was assessed as described above.

Cell transfection. CHO, COS, and RD cells in the exponential phase of growth were trypsinized, washed, and resuspended in electroporation buffer (20 mM HEPES [pH 7.05], 137 mM NaCl, 5 mM KCl, 0.7 mM Na_2HPO_4, 6 mM glucose) at a concentration of 5×10^6 to 1×10^7 cells/ml. Aliquots (500 μl) of the cells were mixed with 75 μg of pEF-BOS (31) containing the cDNA encoding DAF, ICAM-1, or CD36 in electroporation cuvettes (Bio-Rad, Richmond, Calif.) and pulsed at 300 V and 250 μF with a Bio-Rad gene pulser. Cells were then used to seed either 24- or 96-well tissue culture plates and incubated for 48 h at 37°C to form confluent monolayers. The DAF cDNA was obtained from Anthony D'Apice, Clinical Immunology, St. Vincent's Hospital, Melbourne, Victoria, Australia; the ICAM-1 cDNA was obtained from Imperial Cancer Research Fund, David Simmons, John Radcliffe Hospital, Oxford, United Kingdom; and the CD36 cDNA was obtained from Andrew Boyd. Surface protein expression by the transfected cells was monitored by indirect immunofluorescent staining analyzed with a FACStar analyzer (Becton Dickinson, Sydney, New South Wales, Australia) as described previously (38).

Surface biotinylation, chemical cross-linking, and immunoprecipitation. Cells (5×10^6) were detached from the surface of plastic tissue culture flasks by using an EDTA solution and washed once in PBS. Washed cells were resuspended into 3 ml of biotinylation buffer (10 mM sodium borate [pH 8.8], 150 mM NaCl). Biotinamidocaproate *N*-hydroxysuccinimide ester was added to 50 μg/ml, and the sample was placed at room temperature for 15 min. The reaction was terminated by the addition of NH_4Cl to 10 mM. Cells were washed twice in PBS and resuspended in buffer A (138 mM NaCl, 2.9 mM KCl, 0.5 mM $MgCl_2$, 12 mM $NaHCO_3$, 0.3 mM NaH_2PO_4, 5.5 mM glucose, 10 mM HEPES [pH 7.4]). To determine spatial-functional associations within the biotinylated cell membranes, the cells were exposed to the membrane-permeable, cleavable, homobifunctional chemical cross-linking agent DSP (dithiobis [succinimidylpropionate]) (1 mM) for 60 min at room temperature. The reaction was stopped by the addition of Tris-HCl (pH 7.4) to 50 mM. Surface-labeled, cross-linked cells were washed twice in PBS before lysis in buffer B (1% Triton X-100, 150 mM NaCl, 2 mM EDTA, 50 mM Tris-HCl [pH 7.4], 10 μg of soybean trypsin inhibitor per ml, 2 mM phenylmethylsulfonyl fluoride, 20 mM iodoacetamide). Cell lysates were placed on ice for 60 min and then centrifuged at $15,000 \times g$ for 15 min to remove detergent-insoluble material. Soluble lysates were precleared with rabbit anti-mouse immunoglobulin G coupled to Sepharose 4B (RAM-Sepharose). In some experiments, preclearing with transferrin directly coupled to Sepharose 4B was performed in addition to RAM-Sepharose. Specific proteins were then precipitated with the appropriate antibody, followed by RAM-Sepharose. Immune complexes were washed three times with lysis buffer and resolved (reduced) by SDS-polyacrylamide gel electrophoresis. Resolved proteins were electrophoretically transferred to nitrocellulose membranes. Streptavidin-biotin-horseradish peroxidase complexes were used to probe the membrane, and labeled proteins were visualized by using enhanced chemiluminescence (Amersham Life Sciences, Amersham, United Kingdom).

RESULTS

Inhibition of CAV21 cellular attachment by MAb blockade and PI-PLC treatment. To determine whether CAV21 used ICAM-1 as its sole attachment receptor, we investigated CAV21 binding to human carcinoma cell lines that differed in levels of ICAM-1 expression. The fluorescence histograms shown in Fig. 1A indicate that HeLa-B cells express significantly more ICAM-1 than HEp2 cells, while both lines express similar levels of DAF. To analyze these molecules at the level of virus binding, confluent monolayers of each cell line were incubated with purified [^{35}S]methionine-labeled preparations of either E7, which binds DAF (2, 6, 40), HRV14, which binds ICAM-1 (8, 18), or CAV21. As expected, E7 bound equally to both lines, while HRV14 bound to HEp2 cells at only 20% of the level observed for HeLa-B cells (Fig. 1B), reflecting the lower levels of ICAM-1 on this cell line. However, unexpectedly, CAV21 bound equally to both cell lines (Fig. 1B).

To further examine the nature of the CAV21 cell attachment, virus binding following anti-DAF and ICAM-1 MAb blockade was undertaken. The results shown in Fig. 1C, indicate that the anti-DAF SCR3 MAb (IH4) blocked E7 binding, while the anti-ICAM-1 domain MAb (WEHI) significantly reduced HRV14 attachment to HeLa-B cells. Surprisingly, CAV21 binding was unaffected by pretreatment of HeLa-B cells with either MAb. The anti-PVR MAb 280, used as a negative control, was unable to reduce the binding of any of the viruses. These findings suggested that CAV21, in the presence of ICAM-1 receptor blockage, can attach to an alternate receptor.

To investigate whether DAF may play a functional role in CAV21 cell binding, HeLa-B and HEp2 cells were pretreated with PI-PLC. This enzyme cleaves molecules with a glycosylphosphatidylinositol cell anchor, including DAF, releasing them from the cell surface (12). Each cell type was preincubated in the presence or absence of PI-PLC and then incubated with purified [^{35}S]methionine-labeled E7 or CAV21. The data shown in Fig. 2A reveal that PI-PLC treatment abolished E7 binding to both lines; however, whereas CAV21 binding was reduced on HEp2 cells, binding to HeLa-B cells was unaffected. This result suggested that on HeLa-B cells that express high levels of both ICAM-1 and DAF, CAV21 can bind to either molecule, whereas in the absence of DAF on the PI-PLC-treated HEp2 cells, binding is significantly reduced due to a lower level of ICAM-1.

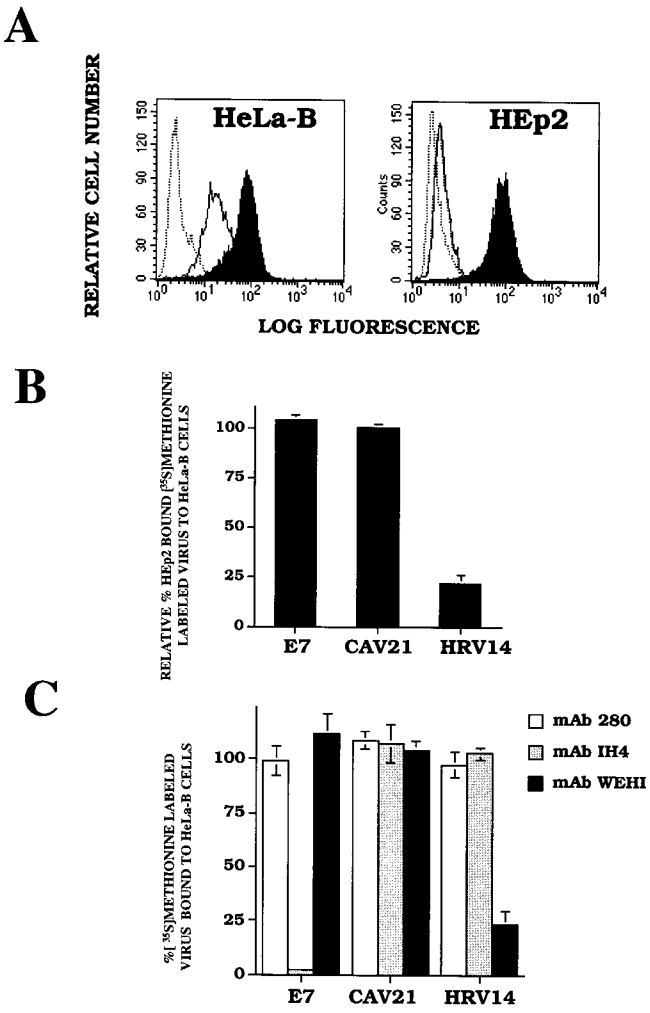

FIG. 1. Anti-DAF and anti-ICAM-1 MAb and viral binding to HeLa-B and HEp2 cells. (A) Flow cytometric analysis of MAb IH4 and MAb WEHI binding to HeLa-B and HEp2 cells. The dotted histogram represents binding of the isotype-matched MAb, the open histogram represents binding of MAb WEHI (anti-ICAM-1), while binding of MAb IH4 (anti-DAF) is shown by the closed histogram. (B) Viral binding to HeLa-B and HEp2 cell monolayers. HEp2 and HeLa-B cell monolayers in 24-well plates were incubated with radiolabeled viruses (3×10^4 to 5×10^4 cpm) in serum-free DMEM for 1 h at 37°C. The amount of virus bound to the cells was determined as described in Materials and Methods. Results are expressed as viral binding to HEp2 cells as a percentage relative to binding for HeLa-B cells ± SD of triplicate wells. (C) Viral binding to HeLa-B cell monolayers pretreated with MAbs 280 (anti-PVR), IH4, and WEHI. HeLa-B cell monolayers in 24-well plates were preincubated with MAbs (20 μg), washed, and then incubated with radiolabeled viruses (2×10^4 to 5×10^4 cpm) as described above. Results are expressed as mean percentage virus bound to HeLa-B cells relative to the no-MAb control ± SD of triplicate wells.

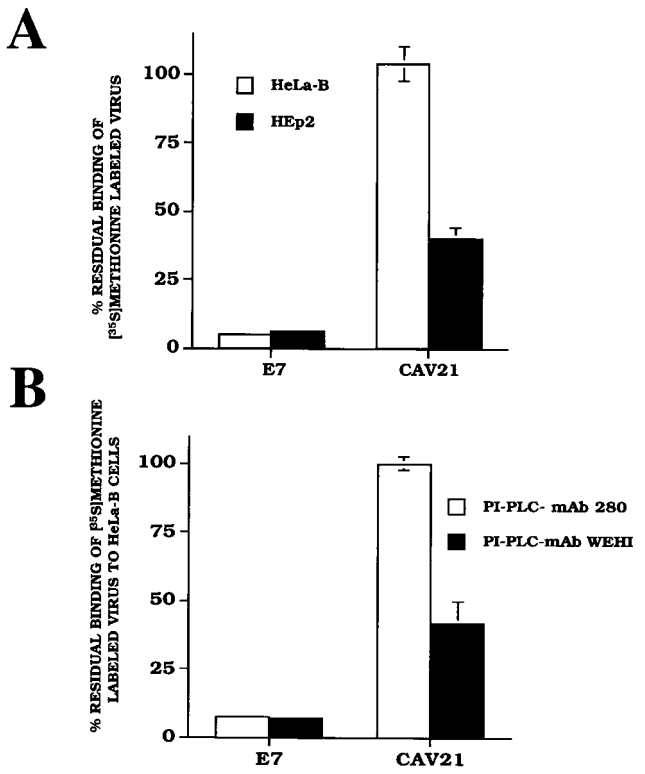

FIG. 2. Viral binding to HeLa-B and HEp2 cells following PI-PLC treatment. (A) E7 and CAV21 binding to HeLa-B and HEp2 cell monolayers preincubated with PI-PLC. HEp2 and HeLa-B cells were incubated with PI-PLC (1.0 U/5×10^6 cells), washed, and then incubated with radiolabeled viruses (2×10^4 to 5×10^4 cpm) in serum-free DMEM for 1 h at 37°C. Results are expressed as the mean percentage of virus bound relative to cell monolayers not pretreated with PI-PLC ± SD of triplicate wells. (B) Antibody blockade of E7 and CAV21 binding to PI-PLC pretreated HeLa-B cells. HeLa-B cells that had been pretreated with PI-PLC as described above were incubated with MAb 280 or WEHI prior to addition of purified [35S]methionine-labeled E7 and CAV21 (2×10^4 to 5×10^4 cpm). The results are expressed as the mean percentage of viral binding relative to the no-MAb control treated cells ± SD of triplicate wells.

To substantiate the notion that CAV21 could bind to either ICAM-1 or DAF on HeLa-B cells, PI-PLC-treated cells monolayers were incubated either with MAb 280 (anti-PVR), as a control, or with MAb WEHI (anti-ICAM-1) prior to exposure to radiolabeled E7 or CAV21. In this instance (Fig. 2B), following the removal of DAF, the anti-ICAM-1 MAb significantly reduced CAV21 binding. As was previously observed, E7 cell attachment was abolished by PI-PLC treatment.

Identification of the CAV21 binding domain on DAF as SCR1. To confirm that CAV21 bound directly to DAF, we measured viral binding to CHO cells transiently expressing either ICAM-1 or DAF. Flow cytometric analysis revealed that approximately 25% of the transfected cell populations expressed detectable levels of either DAF or ICAM-1 (data not shown). The results (Fig. 3) show that CAV21 bound to CHO cells expressing either DAF or ICAM-1.

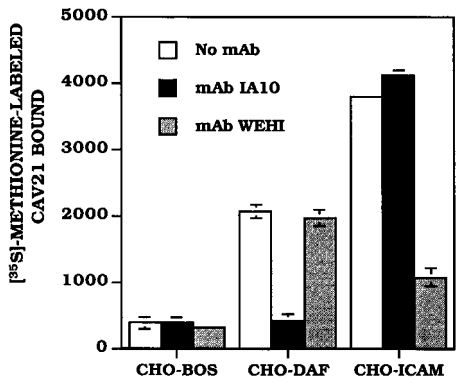

FIG. 3. Transient expression of DAF or ICAM-1 results in binding of CAV21. Confluent monolayers of CHO cells that had been mock transfected (CHO-BOS) or were transiently expressing DAF or ICAM-1 were incubated without antibody or with MAb IA10 (anti-DAF SCR1) or MAb WEHI (20 μg/ml) for 1 h at 37°C prior to addition of purified [35S]methionine-labeled CAV21 (3×10^4 cpm). Results represent the means of triplicate wells ± SD.

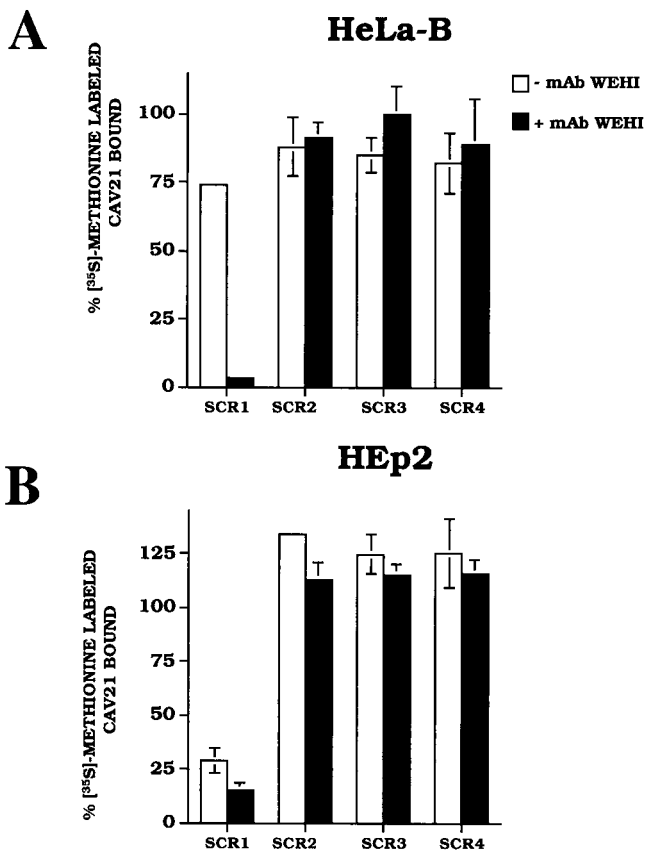

FIG. 4. MAb blockade of CAV21 binding to HeLa-B and HEp2 cells. Confluent monolayers of HeLa-B (A) and HEp2 (B) cells were incubated with anti-DAF MAbs IA10 (SCR1), VIIIA7 (SCR2), IH4 (SCR3), and IIH6 (SCR4) alone or in combination with anti-ICAM-1 MAb (WEHI) prior to addition of purified [^{35}S]methionine-labeled CAV21 (3×10^4 cpm). Results are expressed as the mean percentage of CAV21 bound relative to the no-MAb control ± SD of triplicate wells.

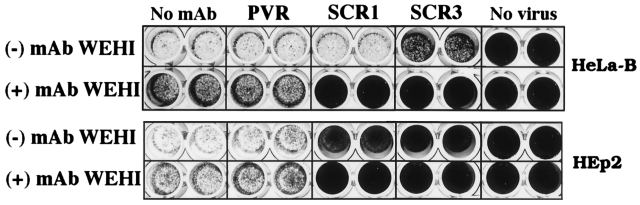

FIG. 5. MAb blockade of CAV21 replication in HeLa-B and HEp2 cells. (A) Confluent monolayers of HeLa-B and HEp2 cells were incubated with anti-PVR MAb 280 and anti-DAF MAbs IA10 (SCR1) and IH4 (SCR3), alone or in combination with anti-ICAM-1 MAb (WEHI), prior to challenge with 10^4 $TCID_{50}$ of CAV21 per well. Following incubation for 48 h at 37°C, cell monolayers were stained and examined for signs of CAV21 cell lysis.

These data established that CAV21, in addition to binding to ICAM-1, can also bind to DAF. Therefore, we used MAb blockade to map the CAV21 binding region on the DAF molecule. An anti-SCR-3 DAF MAb failed to block CAV21 binding to HeLa-B cells (Fig. 1C); therefore, blockade by MAbs to each of the four SCRs of DAF was tested. Following incubation for 48 h, the transfected cells were exposed to radiolabeled CAV21. With the transfected CHO cells, it was found that MAbs to SCR2, 3-, or 4- of DAF did not inhibit CAV21 binding to cells expressing either DAF or ICAM-1 (data not shown). However, a MAb to the SCR1 of DAF (IA10) virtually abolished virus binding to the DAF-expressing cells while having no effect on binding to ICAM-1-expressing cells (Fig. 3). The anti-ICAM-1 MAb inhibited binding to CAV21 only to the cell expressing ICAM-1 and had no effect on viral binding to DAF (Fig. 3).

The MAb directed against the first DAF SCR also partially reduced CAV21 binding to HeLa-B cells and greatly reduced CAV21 binding to HEp2 cells, while the remaining anti-DAF MAbs were ineffective on both cell lines (Fig. 4). The combination of the anti-ICAM-1 MAb together with the anti-DAF SCR1 MAb abolished residual CAV21 attachment to both HeLa-B and HEp2 cells. No other combination of anti-ICAM and anti-DAF MAbs (SCR2-, 3-, or 4-) blocked CAV21 binding to either cell type (Fig. 4). These data indicate that CAV21 binds to either DAF or ICAM-1 and that the DAF binding occurs on a region that is on or proximal to the N-terminal DAF SCR.

Inhibition of CAV21-mediated cell lysis by MAb blockade. Having identified DAF and ICAM-1 as the components of the CAV21 attachment complex on the surface of HEp2 and HeLa-B cells, we investigated the capacity of anti-DAF SCR1 and SCR3 and ICAM-1 domain 1 MAbs to inhibit CAV21 lytic infection. Confluent monolayers of HEp2 and HeLa-B cells in microtiter plates were pretreated with either anti-PVR, anti-DAF (SCR1 or SCR3), or anti-ICAM-1 MAbs or combinations of anti-DAF and anti-ICAM MAbs for 1 h at 37°C before challenge with 10^4 $TCID_{50}$ of CAV21 per well. The results presented in Fig. 5 indicate that the anti-DAF (SCR1) MAb alone provided significant protection to HEp2 cells but not HeLa-B cells. Conversely, the anti-ICAM-1 MAb had little protective effect on HEp2 cells but partially blocked replication on HeLa-B cells. However, as expected from the MAb blockade of binding, the combination of both MAbs afforded high level protection from CAV21 mediated cell lysis in both cell lines. The anti-PVR MAb (280), whether used by itself or in combination with the anti-ICAM-1 MAb, had no effect in blocking CAV21 lytic infection (Fig. 5). Surprisingly, the anti-DAF (SCR3) MAb, whether used alone or in combination with the anti-ICAM-1 MAb, was able to significantly block CAV21 infection on both cell lines (Fig. 5). This result suggested that DAF and ICAM-1 may be coexpressed in close proximity at the cell surface, such that binding of the anti-DAF (SCR3) MAb may form a physical barrier preventing ICAM-1-bound CAV21 interacting with the cell membrane.

DAF and ICAM-1 are spatially associated on the cell surface. To investigate whether DAF and ICAM-1 were expressed in close proximity, HeLa-B cells were surface biotinylated, chemically cross-linked, and immunoprecipitated with anti-DAF and anti-ICAM-1 MAbs (Fig. 6A). In the absence of cross-linking, the anti-DAF MAb immunoprecipitated two polypeptides of 68 and 78 kDa, while the ICAM-1 MAb immunoprecipitated a polypeptide of approximately 90 kDa. The negative control MAb did not recognize any polypeptides corresponding to those identified by either anti-DAF or anti-ICAM-1 MAbs. In all reactions, a band at 87 kDa, probably representing contaminating transferrin receptor (CD71), was seen, and two unidentified bands at 66 and 73 kDa were observed. Following cross-linking, immunoprecipitation with the anti-DAF MAb revealed a polypeptide profile similar to that obtained from non-cross-linked cells. Immunoprecipitation of cross-linked cells with the anti-ICAM-1 MAb identified the ICAM-1 band at 90 kDa also seen in non-cross-linked samples but also revealed an additional polypeptide of 78 kDa, similar to that observed in both DAF MAb immunoprecipitates (Fig. 6A). The fact that no detectable ICAM-1 was observed in the

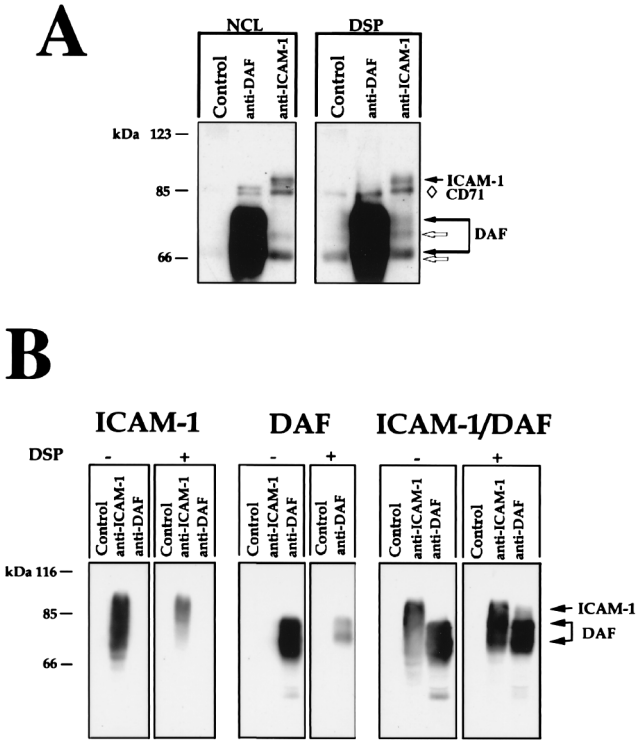

FIG. 6. Immunoprecipitation of surface-expressed DAF and ICAM-1 following chemical cross-linking. (A) HeLa-B cells were surface biotinylated and immunoprecipitated with either an anti-DAF (SCR1) MAb, anti-ICAM-1 MAb, or control MAb (AK7) prior to (non-cross-linked [NLC]) and following (DSP) chemical cross-linking. The immunoprecipitates were separated by SDS-polyacrylamide gel electrophoresis and transferred electrophoretically to nitrocellulose membranes; streptavidin-biotin-horseradish peroxidase complexes were used to probe the membrane, and labeled polypeptides were visualized by using enhanced chemiluminescence (Amersham Life Sciences). The diamond represents the location of contaminating CD71, while the unidentified bands are marked by the open arrowheads. (B) COS cells transiently expressing DAF, ICAM-1, or both were processed as for panel A except that the biotinylated cell lysates were precleared with transferrin coupled to Sepharose CL46 beads to remove contamination by the transferrin receptor (CD71). MAb VM58 (anti-CD36) was used as a negative control.

cross-linked anti-DAF immunoprecipitate from these cells may reflect the fact that as DAF is expressed in much greater levels than ICAM-1 on the surface of HeLa-B cells (Fig. 1A), a large proportion of cell surface DAF is not associated with ICAM-1. Therefore to substantiate that a spatial association exists between DAF and ICAM-1, COS cells transiently expressing comparable levels of either DAF or ICAM-1 or both DAF and ICAM-1 were subjected to the same cross-linking procedure. Following biotinylation and prior to immunoprecipitation, transfected COS lysates were precleared with transferrin-coupled Sepharose beads to remove contaminating CD71 from the immunoprecipitates (Fig. 6B). Anti-ICAM-1 and anti-DAF MAbs identified only polypeptides corresponding to ICAM-1 (a broad band from 80 to 90 kDa) and DAF (bands at 70 and 80 kDa), respectively, from the COS cells cotransfected with DAF and ICAM-1 cDNAs (Fig. 6B). However, following cross-linking of these cells, immunoprecipitation with either anti-ICAM-1 or anti-DAF MAbs identified polypeptides corresponding to both DAF and ICAM-1. These results indicate that DAF and ICAM-1 are coexpressed in close proximity on the cell surface.

Can DAF mediate a productive CAV21 cell infection? To address this question, CHO cells either stably or transiently expressing DAF were inoculated with CAV21 at 1.0 $TCID_{50}$/cell. Observation of cells over a 48-h period postinfection (p.i.) failed to detect cell lysis or changes in cell morphology. Also, titration of CAV21 yields in these cells at 24 h and 48 h p.i. did not detect any increase in CAV21 titer compared to the level observed at 0 h p.i. (data not shown).

This finding may have resulted from the use of hamster cells; therefore, we determined whether a human cell that expressed DAF but not ICAM-1 was susceptible to CAV21 infection. Flow cytometric analysis using anti-DAF and ICAM-1 MAbs indicated that rhadomyosarcoma (RD) cells might be a suitable cell line: although the level of DAF expression on these cells was found to be lower than on HeLa-B cells, ICAM-1 expression was undetectable (Fig. 7A). Therefore, the CAV21 binding capacity of these cells was assessed and compared to that of HeLa-B cells. The data shown in Fig. 7B indicate that CAV21 bound to the surface of RD cells to about 30% of the level observed for HeLa-B cells and that this attachment could be reduced to background levels by pretreatment with an anti-DAF SCR1 MAb. To test for susceptibility to CAV21 infection, confluent monolayers of RD cells in 24-well plates were inoculated with CAV21 (1.0 $TCID_{50}$/cell) and monitored for signs of lysis and changes in cell morphology over a 48-h period. No detectable signs of CAV21-induced cell lysis were observed, and analysis of viral titers at 0, 24, and 48 h p.i. revealed insignificant levels of viral growth (data not shown).

To establish whether the presence of ICAM-1 was the limiting factor in inducing CAV21-mediated cell lysis, RD cells were transfected with either ICAM-1 or CD36 cDNA in the mammalian expression vector pEFBOS or with vector alone. The relative levels of ICAM-1 and CD36 cell surface expression were assessed at 48 h posttransfection by using flow cytometry. Approximately 70% of the transfected RD cells specifically expressed detectable levels of either ICAM-1 or CD36. The control transfectants (pEFBOS) expressed neither antigen, and expression of either ICAM-1 or CD36 had no effect on endogenous DAF expression (data not shown). Confluent monolayers of each of the transfected RD cell populations were inoculated with CAV21 (1.0 $TCID_{50}$/cell) and examined for signs of infection over the next 48 h. As shown in Fig. 7C, the presence of surface-expressed ICAM-1 facilitated virtually complete lysis of the cell monolayer by CAV21, while vector- and CD36-transfected RD cells were unaffected by the virus.

To determine whether DAF played a significant biological role in CAV21-mediated lysis of ICAM-1-expressing RD cells, surface DAF was removed from these cells by treatment with PI-PLC prior to and during infection with CAV21. The fluorescence histograms in Fig. 8A of uninfected cells following the 24-h incubation period at 37°C in the presence or absence of PI-PLC indicate that PI-PLC treatment reduced DAF levels to near background while not affecting the expression of either transfected ICAM-1 or the endogenous PVR. ICAM-1-expressing RD cells preincubated in the presence or absence of PI-PLC were infected with fivefold dilutions of stock preparations of E7, PV2, or CAV21 and following a 24-h incubation period were examined for signs of cell lysis. Viral titration curves (Fig. 8B) indicated that PI-PLC treatment of ICAM-1-expressing RD cells significantly reduced E7-mediated cell lysis, while the lytic effect of PV2 and CAV21 remained unaffected.

DISCUSSION

In this study we show that CAV21 can bind to both DAF and ICAM-1 and that MAbs directed against the N-terminal domains of DAF and ICAM-1 specifically abolished binding to

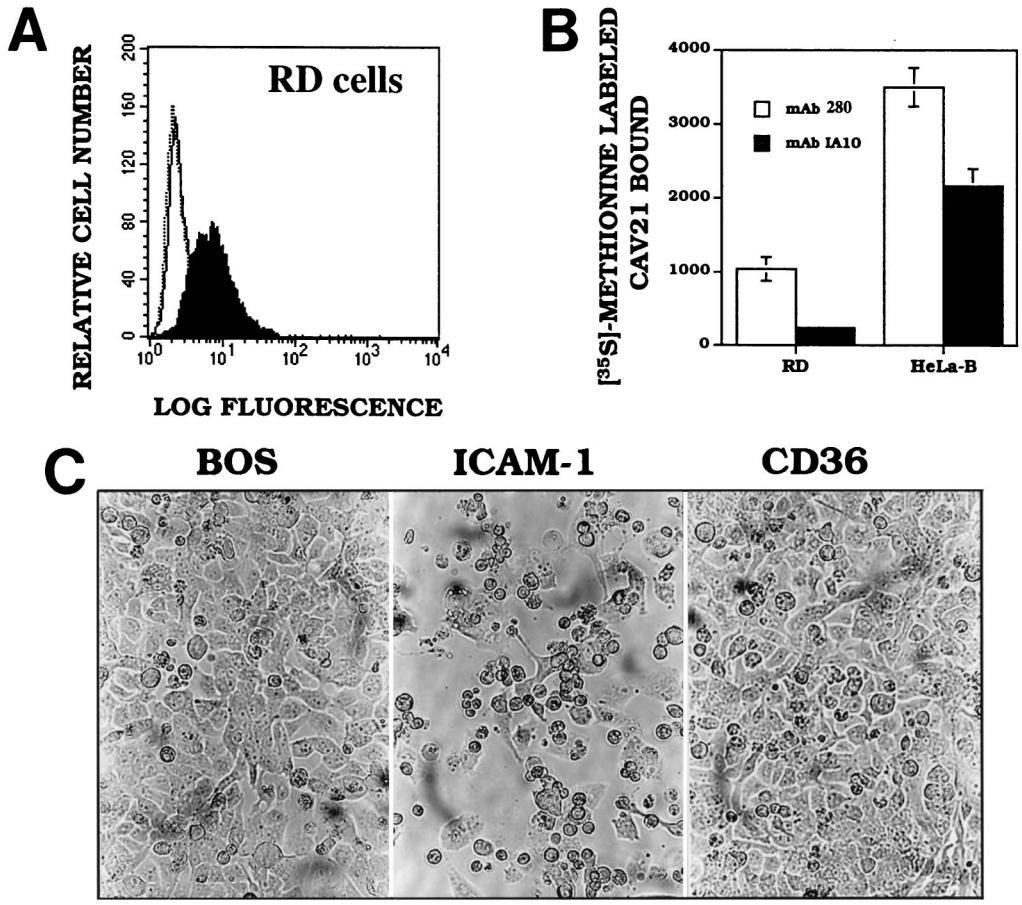

FIG. 7. Binding and infection of rhabdomyosarcoma (RD) cells by CAV21. (A) Flow cytometric analysis of binding of MAbs IA10 and WEHI to RD cells. The dotted histogram represents the binding of the isotype-matched MAb, the open histogram represents the binding of the anti-ICAM-1 MAb (WEHI), and the closed histogram represents the binding of the anti-DAF MAb (IA10). (B) Monolayers of RD and HeLa-B cells were incubated with MAb IA10 or WEHI prior to addition of purified [^{35}S]methionine-labeled CAV21 (2×10^4 cpm). Results represent the means triplicate wells ± SD. (C) CAV21-induced cell lysis of ICAM-1-expressing RD cells. Monolayers of RD cells expressing either ICAM-1 or CD36 were inoculated with CAV21 (1.0 $TCID_{50}$/cell). Following incubation for 48 h at 37°C, the cell monolayers were inspected for signs of cell lysis and then photographed at a magnification of ×20 with Kodak Technical Pan 100 ASA film.

CHO-DAF and CHO-ICAM-1 transfectants, respectively. Individually, these antibodies had little, if any effect on binding of CAV21 to permissive HeLa-B cells (high DAF and ICAM-1 expression), but used in combination, they inhibited viral binding and replication. Interestingly, in this cell line, the anti-ICAM-1 MAb did not reduce viral binding but partially blocked CAV21 lytic infection. Removal of surface DAF from HeLa-B cells by PI-PLC treatment did not reduce CAV21 binding, but subsequent treatment with an anti-ICAM-1 MAb significantly reduced CAV21 attachment. In HEp2 cells (high DAF and low ICAM-1 expression), the anti-SCR1 DAF MAb used alone significantly blocked CAV21 binding and infection. As combinations of the anti-DAF and ICAM-1 MAbs completely block attachment and replication in both HeLa-B and HEp2 cells, these results suggest possible receptor cooperativity between DAF and ICAM-1 in CAV21 cell entry.

The existence of a spatial association between DAF and ICAM-1 was indirectly identified by the capacity of an anti-DAF (SCR3) MAb to significantly block CAV21 infection without reducing cell attachment. It was considered that binding of this MAb to DAF may form a physical barrier preventing ICAM-1-bound CAV21 from penetrating the cell membrane. Subsequent chemical cross-linking investigations confirmed that DAF and ICAM-1 are closely associated on the cell surface. It is interesting that while DAF MAb blockade can block cell infection by CAV21, it had no effect on that of HRV14 (data not shown). Considering that HRV14 and CAV21 compete for the same binding epitope on ICAM-1, and both viruses are conformationally altered following ICAM-1 binding, this finding provides indirect evidence for a functional role of DAF in the cell entry of CAV21. These data confirm and offer an explanation for findings from a previous study, which found that a MAb recognizing a HeLa cell surface protein (now identified as DAF [2]) could block cell infection by CAV21 but not by HRV14 (11).

It was therefore important to determine whether DAF could act independently as an alternate receptor for CAV21 or whether DAF and ICAM-1 functioned together as a receptor complex. To address this question, normally nonpermissive CHO cells were transfected with the cDNA encoding human DAF and were then inoculated with CAV21; cell lysis or evidence of virus growth was not observed. Additionally, low-DAF-expressing rhadomyosarcoma (RD) cells that bound CAV21 were shown to be insusceptible to lytic infection. This was not simply a function of reduced DAF expression, as these cells were refractile to infection when surface DAF levels were increased following transfection with human DAF cDNA (data not shown). However, transfection of these cells with ICAM-1

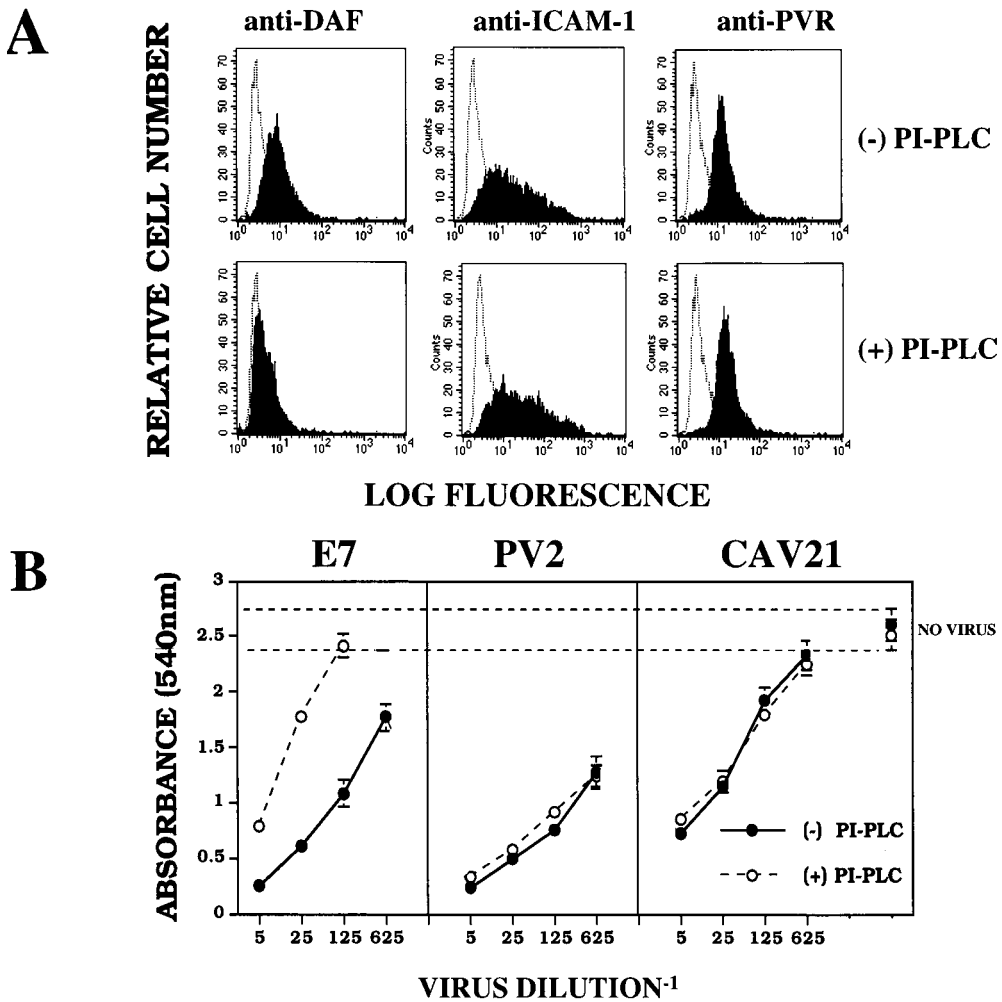

FIG. 8. Replication of E7, PV2, and CAV21 in PI-PLC-treated ICAM-1-expressing RD cells. (A) Flow cytometric analysis of binding of MAbs IA10, WEHI, and 280 to ICAM-1-transfected RD cells pretreated with PI-PLC. The dotted histograms represent the binding of the isotype-matched control MAb, while the closed histograms represent the binding of the anti-DAF (IA10), anti-ICAM-1 (WEHI), and anti-PVR (280) MAbs, as appropriate. (B) Replication of E7, PV2, and CAV21 in PI-PLC-treated ICAM-1-expressing RD cells. ICAM-1-transfected RD cells in microtiter plates that had been preincubated in the presence or absence of PI-PLC were inoculated with fivefold dilutions of stock preparations of E7, PV2, and CAV21. Following incubation for 24 h at 37°C, cell monolayers were stained and cell survival was quantitated as described in Materials and Methods. Results represent mean absorbance readings of triplicate wells ± SD.

cDNA rendered them highly susceptible to CAV21 lytic infection. Interestingly, RD cells have been reported as the cell line of choice for the isolation of group A coxsackieviruses (36) and have previously been shown to support replication of both HRVR14 and CAV21 (11). As the cellular receptor for HRVR14 is ICAM-1, it is probable that some lines of RD cells express ICAM-1, accounting for their susceptibility to CAV21 infection.

To determine whether the coexpression of DAF and ICAM-1 had an additive effect on CAV21 cell infection, levels of cell lysis in ICAM-1-expressing RD cells treated with PI-PLC were assessed. PI-PLC-mediated removal of DAF from these cells had no detectable effect on CAV21- or PV2-induced lytic infection, while E7 infectivity was significantly reduced. These findings indicate that DAF has little effect on ICAM-1-mediated CAV21 cell infection; however, as low levels of DAF may have persisted during the PI-PLC treatment, an involvement of DAF cannot be completely excluded.

The dual receptor binding capacity of CAV21 raises the question as to whether two separate binding sites for DAF and ICAM-1 exist. X-ray crystallographic and electron density mapping studies have indicated that the related enterovirus CBV3 has two predicated canyon-like structures (32). The first, which is not as pronounced as that for the well-characterized rhinoviruses and polioviruses (8, 35), surrounds the pentameric apex of VP1, while the second is a twofold surface depression lined with residues from VP2 and VP3. It has been suggested that the secondary or alternate receptor for CVB3 binds to epitopes within the second canyon-like structure (32). Extrapolating from these findings, it can be postulated that the N terminus of ICAM-1 might dock into the primary capsid canyon of CAV21 (as is the case for HRV14 [8, 29]) and thus initiate a conformational change, leading to cell infection. In the case of DAF, the N terminus of the molecule might bind to an epitope located in the second canyon-like structure, as was postulated for the binding of CVB3 RD variant to DAF (25, 32), but in this case without facilitating a viral conformational change. Studies addressing these questions are under way.

What physiological role, if any, does DAF play in the CAV21 cell entry mechanism? Unlike the cell entry of measles virus, where either CD46 or moesin can independently mediate infection (37), CAV21 cell entry appears to occur only in

the presence of ICAM-1. For a productive cell infection by a human enterovirus, it is generally accepted that a specific receptor-induced conformational change in the viral capsid is required (5, 10, 16, 17, 19). Previously, we have shown that ICAM-1 induces a conformational change in the CAV21 capsid, facilitating entry into mouse cells expressing human ICAM-1 (39). A possible explanation for the apparent inability of DAF to mediate productive cell infection by CAV21, therefore, may be an inability to induce a specific conformational change in the CAV21 capsid. While this remains to be tested, DAF expression is almost ubiquitous throughout the human body (33), and as DAF and ICAM-1 appear to be surface expressed in close proximity, it is reasonable to postulate that DAF may function as an initial low-affinity CAV21 attachment receptor, thereby providing the virus with a sequestration site which may also enhance viral presentation for high-affinity binding to ICAM-1. However, because of the spatial association of DAF and ICAM-1 on the cell surface, a possible indirect role for DAF as a biological scaffold, promoting more efficient presentation of viral binding epitopes on the ICAM-1 molecule, might also be invoked in this process.

ACKNOWLEDGMENTS

We gratefully acknowledge those investigators mentioned in the text for the provision of MAbs and cDNAs that enabled this study to be undertaken. We also thank Lennart Philipson for critical review of the manuscript.

This research was supported by a project grant from the National Health and Medical Research Council of Australia.

REFERENCES

1. **Bergelson, J. M., B. M. Chan, K. R. Solomon, J. N. St. John, and R. W. Finberg.** 1994. Decay-accelerating factor (CD55), a glycosylphosphatidylinositol-anchored complement regulatory protein, is a receptor for several echoviruses. Proc. Natl. Acad. Sci. USA **91:**6245–6249.
2. **Bergelson, J. M., J. G. Mohanty, R. L. Crowell, N. F. St. John, D. M. Lublin, and R. W. Finberg.** 1995. Coxsackievirus B3 adapted to growth in RD cells binds to decay-accelerating factor (CD55). J. Virol. **69:**1903–1906.
3. **Bhat, S., S. L. Spitalnid, F. Gonzales-Scarano, and D. H. Silberberg.** 1991. Galactosyl ceramid or a derivative is an essential component of the neural receptor for human immunodeficiency virus type 1 envelope glycoprotein gp120. Proc. Natl. Acad. Sci. USA **88:**7131–7134.
4. **Boyd, A. W., S. O. Wawryk, G. F. Burns, and J. V. Fecondo.** 1988. Intercellular adhesion molecule-1 (ICAM-1) has a central role in cell-cell contact-mediated immune mechanisms. Proc. Natl. Acad. Sci. USA **85:**3095–3099.
5. **Casasnovas, J. M., and T. M. Springer.** 1994. Pathway of rhinovirus disruption by soluble intercellular adhesion molecule 1 (ICAM-1): an intermediator in which ICAM-1 is bound and RNA is released. J. Virol. **68:**5882–5889.
6. **Clarkson, N. A., R. Kaufman, D. M. Lublin, T. Ward, P. A. Pipkin, P. D. Minor, D. J. Evans, and J. W. Almond.** 1995. Characterization of the echovirus 7 receptor: domains of CD55 critical for virus binding. J. Virol. **69:**5497–5501.
7. **Colonno, R. J., P. L. Callahan, and W. J. Long.** 1986. Isolation of a monoclonal antibody that blocks attachment of the major group of human rhinoviruses. J. Virol. **57:**7–12.
8. **Colonno, R. J., J. H. Condra, S. Mizutani, P. L. Callahan, M. E. Davies, and M. A. Murcko.** 1988. Evidence for the direct involvement of the rhinovirus canyon in receptor binding. Proc. Natl. Acad. Sci. USA **85:**5449–5453.
9. **Coyne, K. E., S. E. Hall, E. S. Thompson, M. A. Arce, T. Kinoshita, T. Fujita, D. J. Anstee, W. Rosse, and D. M. Lublin.** 1992. Mapping of epitopes, glycosylation sites, and complement regulatory domains in human decay accelerating factor. J. Immunol. **149:**2906–2913.
10. **Crowell, R. L., and L. Philipson.** 1971. Specific alteration of coxsackievirus B3 eluted from HeLa cells. J. Virol. **8:**509–515.
11. **Crowell, R. L., A. K. Field, W. A. Schleif, W. L. Long, R. J. Colonno, J. E. Mapoles, and E. A. Eini.** 1986. Monoclonal antibody that inhibits infection of HeLa and rhabdomyosarcoma cells by selected enteroviruses through receptor blockade. J. Virol. **57:**438–445.
12. **Davitz, M. A., M. L. Low, and V. Nussenzweig.** 1986. Release of decay-accelerating factor (DAF) from the cell membrane by phosphatidylinositol-specific-phospholipase C (PI-PLC). J. Exp. Med. **163:**1150–1161.
13. **Deng, H., R. Liu, W. Ellmeier, S. Choe, D. Unutmaz, M. Burkhart, P. Di Marzio, S. Marmon, R. E. Sutton, C. M. Hill, C. B. Davis, S. C. Peiper, T. J. Schall, D. R. Littman, and N. R. Landau.** 1996. Identification of a major co-receptor for primary isolates of HIV-1. Nature **381:**661–666.
14. **Dragic, T., V. Litwin, G. P. Allaway, S. E. Martin, Y. Huang, K. A. Nagashima, C. Cayanan, P. J. Maddon, R. A. Koup, J. P. Moore, and W. A. Paxton.** 1996. HIV-1 entry into $CD4^+$ cells is mediated by the chemokine receptor CC-CKR-5. Nature **381:**667–673.
15. **Feng, Y., C. C. Broder, P. E. Kennedy, and E. A. Berger.** 1996. HIV-1 entry cofactor: functional cDNA cloning of a seven-transmembrane, G protein-coupled receptor. Science **272:**872–877.
16. **Fricks, C. E., and J. M. Hogle.** 1990. Cell-induced conformational change in poliovirus: externalization of the amino terminus of VP1 is responsible for liposome binding. J. Virol. **64:**1934–1945.
17. **Gomez Yafal, A., G. Kaplan, V. R. Racaniello, and J. M. Hogle.** 1993. Characterization of poliovirus conformational alteration mediated by soluble cell receptors. Virology **197:**501–505.
18. **Greve, J. M., G. Davis, A. M. Meyer, C. P. Forte, S. Connolly Yost, C. W. Marlor, M. E. Kamark, and A. McClelland.** 1989. The major human rhinovirus receptor is ICAM-1. Cell **56:**839–845.
19. **Hoover-Litty, H., and J. M. Greve.** 1993. Formation of rhinovirus-soluble ICAM-1 complexes and conformational changes in the virion. J. Virol. **67:**390–397.
20. **Hsiung, G. D.** 1982. Picornaviridae, p. 89–109. *In* Diagnostic virology. Yale University Press, New Haven, Conn.
21. **Hughes, P. J., C. North, P. D. Minor, and G. Stanway.** 1989. The complete nucleotide sequence of coxsackievirus A21. J. Gen. Virol. **70:**2943–2952.
22. **Karnauchow, T. M., D. L. Tolson, B. A. Harrison, E. Altman, D. M. Lublin, and K. Dimmock.** 1996. The HeLa cell receptor for enterovirus 70 is decay accelerating factor (CD55). J. Virol. **70:**5143–5152.
23. **Kinoshita, T., M. E. Medof, R. Silber, and V. Nussenzweig.** 1985. Distribution of decay accelerating factor in the peripheral blood of normal individuals and patients with paroxysmal nocturnal hemoglobinuria. J. Exp. Med. **162:**75.
24. **Lapham, C. K., J. Ouyang, B. Chandrasekhar, N. Y. Nguyen, D. S. Dimitrov, and H. Golding.** 1996. Evidence for cell-surface association between fusin and the CD4-gp120 complex in human cell lines. Science **274:**602–605.
25. **Lindberg, A. M., R. L. Crowell, R. Zell, R. Kandolf, and U. Pettersson.** 1992. Mapping the RD phenotype of the Nancy strain of B3. Virus Res. **24:**187–196.
26. **Lonberg-Holm, K., R. L. Crowell, and L. Philipson.** 1976. Unrelated animal viruses share receptors. Nature **259:**679–681.
27. **Maddon, P. J., A. G. Dalgleish, J. S. McDougal, P. R. Clapham, R. A. Weiss, and R. Axel.** 1986. The T4 gene encodes the AIDS virus receptor and is expressed in the immune system and the brain. Cell **47:**333–348.
28. **Mazurov, A. V., D. V. Vinogradov, T. N. Vlasik, G. F. Burns, and M. C. Berndt.** 1992. Heterogeneity of platelet Fc-receptor-dependent response to activating monoclonal antibodies. Platelets **3:**181–188.
29. **McClelland, A., J. deBear, S. Connonly Yost, A. M. Meyer, C. W. Marlor, and J. M. Greve.** 1991. Identification of monoclonal antibody epitopes and critical residues for rhinovirus binding in domain 1 of ICAM-1. Proc. Natl. Acad. Sci. USA **88:**7993–7997.
30. **Minor, P. D., P. A. Pipkin, D. Hockley, G. C. Schild, and J. W. Almond.** 1984. Monoclonal antibodies which block cellular receptors of poliovirus. Virus Res. **1:**203–212.
31. **Mizushima, S., and S. Nagata.** 1990. pEF-BOS, a powerful mammalian expression vector. Nucleic Acids Res. **18:**5322.
32. **Muckelbauer, J. K., M. Kremer, I. Minor, G. Diana, F. J. Dutko, J. Groarke, P. C. Pevear, and M. G. Rossmann.** 1995. The structure of coxsackievirus B3 at 3.5A resolution. Structure **3:**653–667.
33. **Nicholson-Weller, A., and C. E. Wang.** 1994. Structure and function of decay accelerating factor CD55. J. Lab. Clin. Med. **123:**485–491.
34. **Reed, L. J., and H. A. Muench.** 1938. A simple method of estimating fifty per cent endpoints. Am. J. Hyg. **27:**493–497.
35. **Rossmann, M. G.** 1989. The canyon hypothesis. Hiding the host cell receptor attachment site on a viral surface from immune surveillance. J. Biol. Chem. **264:**14587–14590.
36. **Schmidt, N. J., H. H. Ho, and E. H. Lennette.** 1975. Propagation and isolation of group A coxsackieviruses in RD cells. J. Clin. Microbiol. **2:**183–185.
37. **Schneider-Schaulies, J., L. M. Dunster, R. Schwartz-Albiez, G. Krohne, and V. ter Meulen.** 1995. Physical association of moesin and CD46 as a receptor complex for measles virus. J. Virol. **69:**2248–2256.
38. **Shafren, D. R., R. C. Bates, M. V. Agrez, R. L. Herd, G. F. Burns, and R. D. Barry.** 1995. Coxsackieviruses B1, B3, and B5 use decay-accelerating factor as a receptor for cell attachment. J. Virol. **69:**3873–3877.
39. **Shafren, D. R., D. J. Dorahy, S. J. Greive, G. F. Burns, and R. D. Barry.** 1997. Mouse cells expressing human intercellular adhesion molecule-1 are susceptible to infection by coxsackievirus A21. J. Virol. **71:**785–789.
40. **Ward, T., P. A. Pipkin, N. A. Clarkson, D. M. Stone, P. D. Minor, and J. W. Almond.** 1994. Decay accelerating factor CD55 is identified as the receptor for echovirus 7 using CELICS, a rapid immuno-focal cloning method. EMBO J. **13:**5070–5074.
41. **Wickham, T. J., P. Mathias, D. A. Cheresh, and G. R. Nemerow.** 1993. Integrins $\alpha V\beta 3$ and $\alpha V\beta 5$ promote adenovirus internalization but not virus attachment. Cell **73:**309–319.